Adaptive Transmission with Frequency-Domain Precoding and Linear Equalization over Fast Fading Channels

Hongyang Zhang, Xiaojing Huang, *Senior Member, IEEE*,
and J. Andrew Zhang, *Senior Member, IEEE*

Abstract—In this paper, the emerging orthogonal time frequency space (OTFS) modulation is firstly restructured as a precoded orthogonal frequency division multiplexing (OFDM) system, so that the well established frequency-domain approach can be applied to perform signal in fast fading channels. Then a frequency-domain minimum mean squared error (MMSE) equalizer for OTFS is introduced and its performance is analyzed based on the eigenvalue decomposition of the channel matrix. Inspired by the frequency-domain precoding structure, an adaptive transmission scheme with frequency-domain precoding matrix composed of the eigenvectors of the channel matrix is proposed to improve the system performance under MMSE equalization, and its optimized performance is derived with simple expression. Finally, considering two extreme channel conditions, the lower and upper bounds for the diversity performance of the adaptive transmission scheme are derived. Simulation results show that the proposed adaptive transmission achieves significantly better performance for short signal frames and can work well with imperfect channel state information (CSI). The derived performance bounds can serve as benchmarks for OTFS and other precoded OFDM systems.

Index Terms—Fast fading channel, OTFS, precoded OFDM, diversity, MMSE

I. Introduction

THE emerging next generation communication techniques require higher system capacity and robust diversity performance. To provide high-speed and reliable connections globally, the current communication networks are evolving towards the integrated space and terrestrial networks (ISTNs). In ISTNs, the satellites, aircrafts and vehicles are always in a state of relative motion [1]–[3]. Therefore, the ability for a transmission scheme to cope with fast fading channels due to Doppler effect is critically important for ISTNs and other future communication systems.

Conventional multicarrier transmission schemes, such as orthogonal frequency division multiplexing (OFDM), are prone to intercarrier interference (ICI) caused by Doppler effect in fast fading channels. Therefore, ICI mitigation techniques are necessary, and can be grouped into two categories. The first category focuses on OFDM transmitter design, such as the ICI self cancellation techniques [4], [5]. The other category is ICI cancellation at the receiver, including the efforts on channel estimation and equalization. Kalman filter [6], [7],

H. Zhang, X. Huang and J. Andrew Zhang are with the School of Electrical and Data Engineering, University of Technology Sydney, Ultimo, NSW, 2007, Australia (emails: Hongyang.Zhang-1@student.uts.edu.au, Xiaojing.Huang@uts.edu.au, and Andrew.Zhang@uts.edu.au).

Bayesian methods [8]–[10] and maximum-likelihood (ML) detection [11] have been adopted for channel tracking and estimation. Besides, optimized equalizations are also proposed using soft-Kalman filter [12] and linear minimum mean square error (LMMSE) methods [13]. However, when the Doppler frequency shift is significant and channel coherent time becomes much smaller than the signal frame length, the lack of the capability for achieving full time diversity limits the performance of conventional modulations in such fast fading channels.

The orthogonal time frequency space (OTFS) modulation shows outstanding performance in fast fading channels [14], [15]. Previous research has demonstrated that OTFS can exploit both time and frequency diversity since it modulates the signals in delay-Doppler domain with inverse symplectic finite Fourier transform (ISFFT). Recent works are mainly focused on the development of estimation and equalization algorithms, such as Markov chain Monte Carlo (MCMC) in [16], message passing (MP) in [17]–[20] and LMMSE in [21]–[24]. Existing studies have disclosed the performance of OTFS systems with the applications of high-complexity and optimal maximal likelihood (ML) detectors [25]–[27]. However, the study on low-complexity and more practical linear equalizers for OTFS is still very limited, not to mention further analytical performance characterization for these equalizers.

In this paper, we propose an adaptive transmission based on frequency-domain precoding and minimum mean square error (MMSE) equalization, which can be used as a general solution to communications over fast fading channels, including OTFS, and conduct detailed performance analysis of it. We first review the representations of fast fading channels in different domains. The frequency-domain received signal model is adopted due to its concise stripe diagonal structure of the frequency-Doppler domain channel matrix. We then formulate OTFS as a more general precoded OFDM system so that the low-complexity frequency-domain approach can be applied to analyze its performance. Note that many conventional modulations can also be regarded as a kind of precoded OFDM, such as the single carrier system with frequency domain equalization (SC-FDE). Although OTFS can achieve full diversity in both time and frequency domains using ML equalization, the high complexity of ML algorithm makes it infeasible in practical application. Therefore, we introduce a more practical frequency-domain MMSE equalization with much lower computational complexity compared with time-domain MMSE

and iterative equalizers such as the MP. To optimize the system performance, we design the precoding matrix based on the eigenvalue decomposition of the channel matrix so that an adaptive transmission is obtained. Simulation results demonstrate that even with imperfect channel state information (CSI) feedback, the adaptive transmission still achieves better performance than OTFS evaluated under both 4-quadrature amplitude modulation (QAM) and 16-QAM schemes. The bit-error-rate (BER) lower bound and upper bound are also derived for the proposed adaptive transmission under two extreme channel conditions, taking into consideration of significantly large numbers of multipaths and Doppler frequency shifts. The main contributions of this paper are summarized as follows.

- First, a frequency-domain signal model with circular stripe diagonal frequency-Doppler domain channel matrix is derived for arbitrary multipath delays and Doppler shifts. This model enables low complexity equalizers to be developed to combat fast channel fading, paving the way for deploying new modulation techniques such as OTFS in practical systems for high mobility applications.
- Second, OTFS is proved to be equivalent to a general precoded OFDM scheme as many other conventional modulations are. This allows well-established receiver design and performance analysis techniques for precoded OFDM to be applied to OTFS.
- Third, an adaptive transmission scheme is proposed to optimize the system performance with the knowledge of CSI. Even with imperfect channel estimation, the adaptive transmission still outperforms OTFS under the same MMSE equalization. This method also achieves significant improvement over conventional OFDM and SC-FDE, which use shorter transmission frames than those of OTFS.
- Fourth, closed-form lower and upper performance bounds are derived for the adaptive transmission to show the theoretical limits of the MMSE equalization over fast fading channels. These bounds provide guidelines for transmission system design and also set up the benchmarks for OTFS system performance analysis.

The rest of the paper is organized as follow. In Section II, the fast fading channel representation in frequency-Doppler domain is developed and the OTFS modulation is formulated as a precoded OFDM system. In Section III, the performance of OTFS under MMSE equalization is analyzed, using a general frequency-domain approach. In Section IV, the optimized adaptive transmission is proposed and the theoretical BER lower and upper bounds are derived. Simulation results are provided in Section V to verify the theoretical analyses and to compare the performance among the proposed adaptive transmission and other conventional systems. Finally, conclusions are drawn in Section VI.

II. CHANNEL AND SYSTEM MODELS

In this section, different channel representations in fast fading channels are first developed. Then, OTFS modulation is reviewed and recast as a precoded OFDM system, enabling low-complexity equalization and closed-form performance analysis.
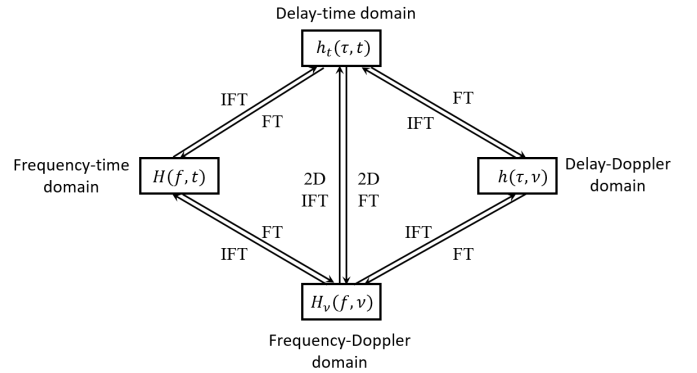

Fig. 1. Relationships among channel representations in different domains.

A. Fast Fading Channel Models

In fast fading channels, both the time delays and the Doppler frequency shifts in multipath environment affect the transmission performance. Assuming a single-input-single-output (SISO) system, the received signal in the continuous-time domain can be expressed as

$$r(t) = \int_{-\infty}^{+\infty} \int_{-\infty}^{+\infty} h(\tau, \nu) s(t - \tau) e^{\mathbf{j}2\pi\nu t} d\tau d\nu + w(t),$$
(1)

where $s(t)$ is the transmitted signal, $h(\tau, \nu)$ is the *delay-Doppler spreading function* of the fast fading channel, $\mathbf{j} = \sqrt{-1}$ and $w(t)$ is the additive white Gaussian noise (AWGN). For a sparse P-path channel, $h(\tau, \nu)$ is defined as

$$h(\tau, \nu) = \sum_{i=1}^{P} h_i \delta(\tau - \tau_i)\delta(\nu - \nu_i),$$
(2)

where h_i, τ_i, and ν_i are the path gain, delay and Doppler shift of the i-th path, respectively, and $\delta(\cdot)$ denotes the Dirac delta function. According to the above delay-Doppler channel model, we can also derive the representations of the fast fading channel in other domains with the help of Fourier transform (FT) and inverse Fourier transform (IFT). Applying IFT to $h(\tau, \nu)$ with respect to the Doppler frequency shift ν, the *delay-time* channel representation can be expressed as

$$h_t(\tau, t) = \int_{-\infty}^{+\infty} h(\tau, \nu)e^{\mathbf{j}2\pi\nu t} d\nu.$$
(3)

Applying FT to $h(\tau, \nu)$ with respect to delay τ, the *frequency-Doppler* representation can be expressed as

$$H_\nu(f, \nu) = \int_{-\infty}^{+\infty} h(\tau, \nu)e^{-\mathbf{j}2\pi f\tau} d\tau.$$
(4)

Applying FT and IFT to $h(\tau, \nu)$ with respect to τ and ν respectively, the *frequency-time* representation can be expressed as

$$H(f, t) = \int_{-\infty}^{+\infty} \int_{-\infty}^{+\infty} h(\tau, \nu)e^{\mathbf{j}2\pi\nu t}e^{-\mathbf{j}2\pi f\tau} d\tau d\nu.$$
(5)

The relationships among the channel representations in different domains are depicted in Fig. 1.

Applying FT to $r(t)$ in (1), the frequency-domain received signal can be modeled as

$$R(f) = \int_{-\infty}^{+\infty} r(t)e^{-\mathbf{j}2\pi ft}dt + W(f)$$

$$= \int_{-\infty}^{+\infty} \int_{-\infty}^{+\infty} H(f',t)e^{-\mathbf{j}2\pi(f-f')t}dtS(f')df' + W(f)$$

$$= \int_{-\infty}^{+\infty} H_\nu(f', f - f')S(f')df' + W(f), \quad (6)$$

where $S(f)$ is the FT of $s(t)$ and $W(f)$ is the AWGN in the frequency domain.

In the discrete-time domain, the transmitted signal can be expressed as $s[i] = s(id_r)$, $i = 0, 1, ..., MN - 1$, where d_r is the *delay resolution* or the sampling period. Assuming that the maximum delay in the multipath channel is d_{max}, the maximum number of resolvable multipaths can be expressed as $L_{max} = \lceil d_{max}/d_r \rceil$, where $\lceil \cdot \rceil$ denotes the ceiling function to obtain the rounded up number, with the required minimum channel bandwidth of $1/d_r$. Denoting f_r as the *Doppler resolution* and f_{max} as the maximum Doppler frequency shift, the maximum number of positive resolvable Doppler frequencies can be expressed as $K_{max} = \lceil f_{max}/f_r \rceil$ over a minimum frame length of $1/f_r$ for the transmitted signals. Note that there are both positive and negative Doppler frequency shifts in the fast fading channel, which means that the Doppler resolution range is $[-K_{max}, K_{max}]$.

In this paper, we concentrate on the system analysis in the frequency-domain. From (4), the discrete frequency-Doppler domain channel representation can be expressed as

$$H_\nu[i, j] = H_\nu(if_\Delta, \bar{v}_j) = \int H(i\Delta f, t)e^{-\mathbf{j}2\pi\bar{v}_jt}dt, \quad (7)$$

Here, f_Δ denotes the subcarrier frequency spacing and $\bar{v}_j$ is the j-th quantized Doppler frequency. Denoting the transmitted and received signal sequences in the discrete-frequency domain as $\mathbf{S}$ and $\mathbf{R}$ respectively, the discrete-frequency domain received signal can be expressed from (6) in matrix form as

$$\mathbf{R} = \mathbf{H}_\nu\mathbf{S} + \mathbf{W}, \quad (8)$$

where $\mathbf{W}$ denotes the frequency-domain noise vector and $\mathbf{H}_\nu$ is the frequency-Doppler domain channel matrix expressed as

$$\mathbf{H}_\nu = \begin{bmatrix} H_\nu[0,0] & \cdots & H_\nu[MN-1,1] \\ H_\nu[0,1] & \cdots & H_\nu[MN-1,2] \\ \vdots & \ddots & \vdots \\ H_\nu[0,MN-1] & \cdots & H_\nu[MN-1,0] \end{bmatrix}. \quad (9)$$

Through (7), (5) and (2), $H_\nu[i, j]$ can be obtained given arbitrary h_i, τ_i and ν_i in any sparse P-path channel.

Fig. 2 shows the construction of (9), in which the shaded squares show the non-zero elements in the matrix, whereas the blank squares show the zero elements. Note that, due to the discretization of $H_\nu(f', \nu)$ as shown in (7), $H_\nu[i, j]$ is periodical in the Doppler domain represented by the index j. When the Doppler frequency shift ν is confined in $[-K_{max}, K_{max}]$, after the coordination transform $\nu = f - f'$, the Doppler shift values appear in the diagonal stripe of width $2K_{max} + 1$ on the f-f' plane. We observe that the frequency-Doppler domain

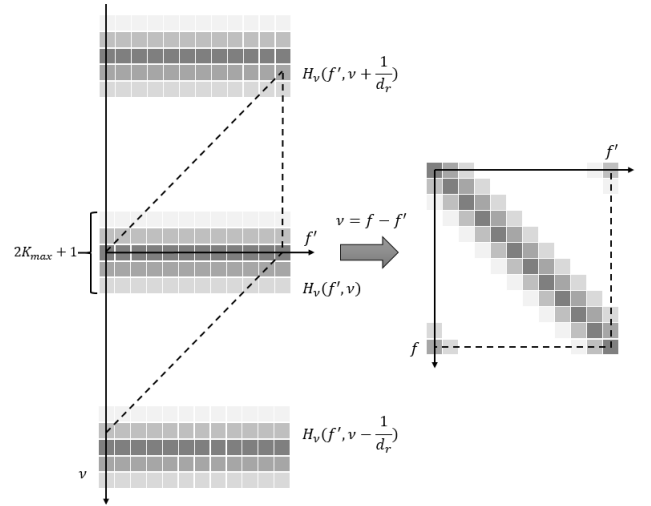
Fig. 2. Construction of channel matrix $\mathbf{H}_\nu$ from $H_\nu[i,j]$.

channel matrix demonstrates a stripe diagonal structure with stripe width $2K_{max} + 1$. This stripe diagonal structure can reduce the receiver signal processing complexity significantly. Similar characteristic in the frequency-domain channel model for OFDM system has also been reported in [28] without explicitly linking the channel matrix to the frequency-time domain channel representation. Therefore, the conventional channel model, such as the one in [28], is only suitable for on-grid path delays and Doppler shifts.

B. OTFS as Precoded OFDM

In the original OTFS system, the data symbols after constellation mapping are arranged in a two dimensional (2D) $M \times N$ matrix $\mathbf{X}$ [14], where M denotes the number of elements in delay dimension, N denotes the number of elements in Doppler dimension, and $\mathbf{X} \in \mathbb{C}^{M \times N}$. In vector form, the data symbols to be transmitted can be expressed as $\mathbf{x} = vec(\mathbf{X})$ where $vec(\cdot)$ is the vectorizing function. After ISFFT, Heisenberg transform and the pulse shaping, the time-domain signal is transmitted through the fast fading channel. Assuming the pulse shaping operation is a rectangular window function, the signal matrix to be sent into the channel can be expressed as

$$\mathbf{D} = \mathbf{F}_M^{\mathbf{H}}(\mathbf{F}_M\mathbf{X}\mathbf{F}_N^{\mathbf{H}}) = \mathbf{X}\mathbf{F}_N^{\mathbf{H}}, \quad (10)$$

where $\mathbf{D}$ is an $M \times N$ matrix, $\mathbf{F}_N$ denotes N-point FFT matrix. The time-domain signal to be transmitted is the vectorized data matrix $\mathbf{D}$ expressed as

$$\mathbf{s} = vec(\mathbf{D}) = (\mathbf{F}_N^{\mathbf{H}} \otimes \mathbf{I}_M)\mathbf{x}, \quad (11)$$

where $\mathbf{s}$ is an $MN \times 1$ vector, $\otimes$ denotes Kronecker product. From (8) and (11), the received frequency-domain signal can be expressed as

$$\mathbf{R} = \mathbf{H}_\nu\mathbf{F}_{MN}(\mathbf{F}_N^{\mathbf{H}} \otimes \mathbf{I}_M)\mathbf{x} + \mathbf{W}. \quad (12)$$

According to the Cooley-Tukey general factorization, the MN-point discrete Fourier transform (DFT) $\mathbf{F}_{MN}$ can be
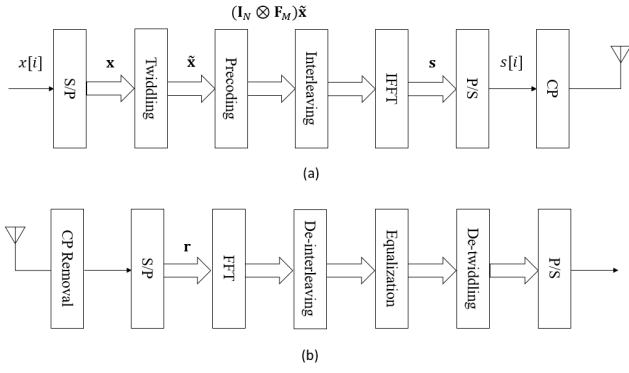
Fig. 3. OTFS system block diagram in precoded OFDM form: (a) transmitter and (b) receiver. S/P and P/S stand for serial-to-parallel and parallel-to-serial conversions respectively, and CP stands for cyclic prefix.

factorized as two smaller DFTs in terms of sizes M and N, which can be expressed as

$$\mathbf{F}_{MN} = \mathbf{P}_{M,N}(\mathbf{I}_N \otimes \mathbf{F}_M)\mathrm{diag}(e^{-\mathbf{j}\frac{2\pi}{MN}(i)_M \lfloor \frac{i}{M} \rfloor})(\mathbf{F}_N \otimes \mathbf{I}_M), \tag{13}$$

where $\mathrm{diag}(x_i)$, $i = 0, ..., MN-1$, denotes a diagonal matrix with the i-th diagonal element x_i, $(\cdot)_M$ denotes modulo M operation, $\lfloor \cdot \rfloor$ denotes flooring operation and $\mathbf{P}_{M,N}$ denotes a permutation matrix of dimension $MN \times MN$. The permutation matrix equivalently performs the interleaving operation that reads the elements in the matrix column-wise and stacks them to a matrix row-wise. Therefore, based on (12) and (13), the received frequency-domain signal becomes

$$\mathbf{R} = \mathbf{H}_\nu \mathbf{P}_{M,N}(\mathbf{I}_N \otimes \mathbf{F}_M)\mathrm{diag}(e^{-\mathbf{j}\frac{2\pi}{MN}(i)_M \lfloor \frac{i}{M} \rfloor})\mathbf{x} + \mathbf{W} \tag{14}$$

and the OTFS system can be transformed into a precoded OFDM system as illustrated in Fig. 3, where $(\mathbf{I}_N \otimes \mathbf{F}_M)$ is the precoding matrix, which is also an unitary matrix, and $\tilde{\mathbf{x}} = \mathrm{diag}(e^{-\mathbf{j}\frac{2\pi}{MN}(i)_M \lfloor \frac{i}{M} \rfloor})\mathbf{x}$ is the twiddled signal vector. Note that the twiddling will only affect the phase of the symbol, and will not affect the signal detection and the BER performance after de-twiddling at the receiver. Excluding the twiddling at the transmitter and the de-twiddling at the receiver, Fig. 3 shows a typical precoded OFDM system [29]. The similarity between these two modulations allows us to use well developed methods in the diversity and performance bound analyses, which can be equally applied to both OTFS and precoded OFDM. Note that the precoded OFDM has demonstrated superb frequency diversity over frequency-selective slow fading channels in previous research works, but its performance over fast fading channels has not been explored yet. The analysis in the following section will show that the precoded OFDM, or similarly the OTFS, is also capable of achieving full time diversity.

III. OTFS PERFORMANCE ANALYSIS

In this section, the diversity performance of OTFS is analyzed with ML and linear equalization respectively.

A. Diversity with ML Equalization

To recover the signal at the receiver, two main categories of equalization techniques can be adopted. The first class is the maximum likelihood sequence estimation (MLSE), which is based on Viterbi algorithm and the Maximum *A Posteriori* Probability (MAP) detection. It is the optimal equalization method to recover the corrupted signals, but it has significant computational complexity exponential to the channel memory length. The second class is the linear equalization such as zero forcing (ZF) and MMSE, which has much lower complexity but the performance is also degraded.

We first analyze the diversity performance of OTFS based on ML equalization. Assuming the CSI is perfectly known at the receiver, the ML estimate of the data symbol $\mathbf{x}$ can be obtained by minimizing

$$(\mathbf{R} - \mathbf{H}_\nu \mathbf{F}_{MN}(\mathbf{F}_N^{\mathbf{H}} \otimes \mathbf{I}_M)\hat{\mathbf{x}})^{\mathbf{H}}(\mathbf{R} - \mathbf{H}_\nu \mathbf{F}_{MN}(\mathbf{F}_N^{\mathbf{H}} \otimes \mathbf{I}_M)\hat{\mathbf{x}}), \tag{15}$$

through exhaustive search from all possible data vectors $\hat{\mathbf{x}}$ [30]. The results in [25]–[27] show that OTFS can achieve full diversity through symbol rotation. Here, we characterize the diversity from another perspective. Assuming the received signal in the time-domain at the receiver is $\mathbf{y}$, we can obtain the received signal-to-noise ratio (SNR) through separately analyzing the signal and noise powers in $\mathbf{E}\{\mathbf{yy^H}\}$. Except for a constant scaling factor, the received SNR can be expressed as

$$\gamma \propto \sum_{l=0}^{L-1} \sum_{k=-K_{max}}^{K_{max}} |h[l,k]|^2 \cdot \frac{\sigma_s^2}{\sigma_w^2}. \tag{16}$$

where σ_s^2 is the transmitted signal power, σ_w^2 is the noise power, $h[l,k]$ is the discrete-time form of $h(\tau,\nu)$, sampled at $\tau = ld_r$ and $\nu = kf_r$ for $l = 0, 1, ..., L-1$, $k = -K_{max}, ..., K_{max}$. The derivation is provided in Appendix A.

Therefore, the received SNR is proportional to the sum of $L \times (2K_{max} + 1)$ random variables $|h[l,k]|^2$, from which we can deduce that OTFS has the potential to achieve full diversity in both time and frequency domain if all the random variables are independent.

B. Performance Analysis for Linear Equalization

Although MLSE equalization can achieve optimal performance, its complexity restricts its practical application. Since linear equalization can be implemented with low complexity in the frequency-domain, it is preferable in practice. In this paper, the MMSE algorithm is adopted as the equalization technique and its output SNR analysis is conducted in the frequency-domain.

Assuming the CSI is perfectly known at the receiver, an estimate of the transmitted signal in the discrete frequency-domain can be expressed as

$$\hat{\mathbf{S}} = \mathbf{G}_\nu \mathbf{R} = \mathbf{G}_\nu \mathbf{H}_\nu \mathbf{S} + \mathbf{G}_\nu \mathbf{W}, \tag{17}$$

where $\mathbf{G}_\nu$ is the equalization matrix expressed as

$$\mathbf{G}_\nu = \mathbf{H}_\nu^{\mathbf{H}}(\mathbf{H}_\nu \mathbf{H}_\nu^{\mathbf{H}} + \frac{1}{\gamma_{in}}\mathbf{I}_{MN})^{-1}, \tag{18}$$

γ_{in} denotes the input SNR at the receiver. Assume that the total number of data symbols to be transmitted is $M \times N$ and let $\mathbf{x} = (x[0], x[1], ..., x[MN - 1])^T$ denote the data symbol vector after the QAM symbol mapping. Let $\mathbf{S} = \mathbf{F}_{MN}\mathbf{V}\mathbf{x}$ where $\mathbf{V}$ and $\mathbf{V}^{\mathbf{H}}$ denote the general modulation and demodulation matrices under the precoded-OFDM system structure, respectively, satisfying $\mathbf{V}\mathbf{V}^{\mathbf{H}} = \mathbf{V}^{\mathbf{H}}\mathbf{V} = \mathbf{I}_{MN}$. A general representation of the received signals after MMSE equalization is given by

$$
\begin{aligned}
\mathbf{y} &= \mathbf{V}^{\mathbf{H}}\mathbf{F}_{MN}^{\mathbf{H}}\hat{\mathbf{S}} \\
&= \mathbf{V}^{\mathbf{H}}\mathbf{F}_{MN}^{\mathbf{H}}\mathbf{G}_{\nu}\mathbf{H}_{\nu}\mathbf{F}_{MN}\mathbf{V}\mathbf{x} + \mathbf{V}^{\mathbf{H}}\mathbf{F}_{MN}^{\mathbf{H}}\mathbf{G}_{\nu}\mathbf{W}.
\end{aligned} \quad (19)
$$

Different modulation schemes can be realized by selecting different $\mathbf{V}$ matrices. To be specific, when $N = 1$, $\mathbf{V} = \mathbf{F}_{M}^{\mathbf{H}}$ represents OFDM signals, and $\mathbf{V} = \mathbf{I}_M$ represents SC-FDE signals. When $N > 1$, $\mathbf{V} = \mathbf{F}_{N}^{\mathbf{H}} \otimes \mathbf{I}_M$ represents OTFS signals. Note that, for different modulations, frame lengths and the sizes of channel matrices may be different. Here, the modulations are divided into two cases, i.e., the long-frame symbol modulation, such as OTFS with frame length MN and $MN \times MN$ channel matrix, and short-frame modulations, such as OFDM and SC-FDE with frame length M and $M \times M$ channel matrix.

Defining $\mathbf{A} = \mathbf{V}^{\mathbf{H}}\mathbf{F}_{MN}^{\mathbf{H}}\mathbf{G}_{\nu}\mathbf{H}_{\nu}\mathbf{F}_{MN}\mathbf{V}$ and using (18), we can obtain

$$
\begin{aligned}
\mathbf{A} &= \mathbf{V}^{\mathbf{H}}\mathbf{F}_{MN}^{\mathbf{H}}\mathbf{H}_{\nu}^{\mathbf{H}}(\mathbf{H}_{\nu}\mathbf{H}_{\nu}^{\mathbf{H}} + \frac{1}{\gamma_{in}}\mathbf{I})^{-1}\mathbf{H}_{\nu}\mathbf{F}_{MN}\mathbf{V} \\
&= (\mathbf{I} + \frac{1}{\gamma_{in}}(\mathbf{V}^{\mathbf{H}}\mathbf{F}_{MN}^{\mathbf{H}}\mathbf{H}_{\nu}^{\mathbf{H}}\mathbf{H}_{\nu}\mathbf{F}_{MN}\mathbf{V})^{-1})^{-1}.
\end{aligned} \quad (20)
$$

Note that $\mathbf{H}_{\nu}^{\mathbf{H}}\mathbf{H}_{\nu}$ is a Hermitian matrix so that it can be expressed using eigenvalue decomposition as

$$
\mathbf{H}_{\nu}^{\mathbf{H}}\mathbf{H}_{\nu} = \mathbf{Q}\mathbf{\Lambda}\mathbf{Q}^{\mathbf{H}}, \quad (21)
$$

where $\mathbf{Q}$ is a square $MN \times MN$ unitary matrix and $\mathbf{\Lambda}$ is a diagonal matrix with the i-th diagonal element λ_i for $i = 0, 1, ..., MN - 1$. Further denoting $\mathbf{U} = \mathbf{V}^{\mathbf{H}}\mathbf{F}_{MN}^{\mathbf{H}}\mathbf{Q}$, we can simplify $\mathbf{A}$ as

$$
\begin{aligned}
\mathbf{A} &= (\mathbf{I} + \frac{1}{\gamma_{in}}\mathbf{U}\mathbf{\Lambda}^{-1}\mathbf{U}^{\mathbf{H}})^{-1} \\
&= \mathbf{I} - \mathbf{U}\text{diag}(\frac{1}{\gamma_{in}\lambda_i + 1})\mathbf{U}^{\mathbf{H}}.
\end{aligned} \quad (22)
$$

According to the MMSE equalization principle, the normalized noise power for the $(nM + m)$-th equalized data symbol can be expressed as

$$
\begin{aligned}
J_{nM+m} &= 1 - \mathbf{A}[nM + m, nM + m] \\
&= \sum_{i=0}^{MN-1} \frac{1}{\gamma_{in}\lambda_i + 1}|\mathbf{U}[nM + m, i]|^2.
\end{aligned} \quad (23)
$$

Therefore, the output SNR for the $(nM + m)$-th data symbol after equalization can be expressed as

$$
\gamma_{out}[m, n] = \frac{1 - J_{nM+m}}{J_{nM+m}} = \frac{1}{J_{nM+m}} - 1. \quad (24)
$$

Based on $\gamma_{out}[m, n]$ and assuming QAM modulation for data symbols, the average BER probability P_b for a given

channel realization can be evaluated for various modulation levels [29] [30] [31]. Averaging over all possible fading channel realizations, the ergodic BER for the fast fading channel is expressed as $E_h\{P_b\}$, where $E_h\{\cdot\}$ denotes the ensemble average over all delay-Doppler channel realizations.

From (24), the output SNR depends on the $\mathbf{U}$ matrix which in turn depends on the modulation method $\mathbf{V}$ and the channel matrix $\mathbf{H}_{\nu}$. If $\mathbf{V}$ is not adaptive to $\mathbf{H}_{\nu}$, the equalization performance is obviously not optimized. Inspired by the similarity between OTFS and precoded OFDM, we propose an adaptive transmission strategy based on the eigenvalue analysis of the channel to further optimize the transmission performance and derive the BER bounds in the fast fading channels in the following section.

IV. ADAPTIVE TRANSMISSION AND BER BOUNDS

In this section, a novel adaptive transmission scheme is proposed based on frequency-domain precoding and MMSE equalization. Then, the BER upper and lower bounds are analyzed under different extreme channel conditions.

A. Adaptive Transmission

As can be seen from (23), after frequency-domain MMSE equalization, the normalized noise power for each data symbol is generally different from each other and affected by the modulation matrix V and the unitary matrix Q obtained from channel matrix eigenvalue decomposition. Assuming that the CSI can be fed-back to the transmitter, we can adaptively determine the modulation matrix V based on the channel conditions to reduce the normalized noise power and hence improve the output SNR of the equalization, resulting in an adaptive transmission system. This can be achieved by constructing the modulation matrix $\mathbf{V}$ such that $\mathbf{U}$ satisfies

$$
|\mathbf{U}[nM + m, i]|^2 = \frac{1}{MN}, \quad (25)
$$

and the normalized noise power for the equalized data symbol becomes

$$
J = \frac{1}{MN} \sum_{i=0}^{MN-1} \frac{1}{\gamma_{in}\lambda_i + 1}, \quad (26)
$$

which is the same for all the data symbols. Therefore, the optimized output SNR can be simplified as

$$
\gamma_{out}^{*} = \frac{1}{\dfrac{1}{MN} \displaystyle\sum_{i=0}^{MN-1} \dfrac{1}{\gamma_{in}\lambda_i + 1}} - 1. \quad (27)
$$

For a general precoded OFDM system, Eqs. (23) and (24) show that the output SNR is related to the input SNR, eigenvalues of the channel, and the parameter $\mathbf{U}$, which can be affected by the modulation method $\mathbf{V}$ and unitary matrix $\mathbf{Q}$ of the channel. However, after applying the adaptive transmission, $\mathbf{U}$ is transformed to an IFFT matrix with constant magnitude elements as shown in (25), and the output SNR is simplified as shown in (27). Under this adaptive modulation, only the input SNR and eigenvalues of the channel can affect the output
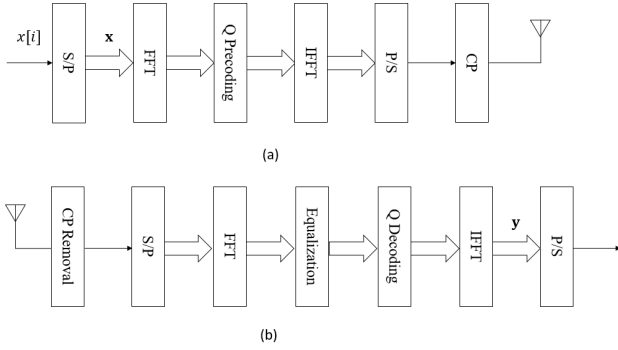
Fig. 4. Adaptive transmission system block diagram: transmitter (a) and receiver (b).

SNR. Moreover, note that the denominator of (27) is a sum of $\frac{1}{\gamma_{in}\lambda_i+1}$, because MMSE equalizer instead of zero forcing is used here. Even if some channels have some zero eigenvalues, no singularity will happen and the performance will not break down. Therefore, the adaptive transmission is feasible under all channel conditions.

Letting $\mathbf{V} = \mathbf{F}_{MN}^{\mathbf{H}}\mathbf{Q}\mathbf{F}_{MN}$ and substituting it into $\mathbf{U}$, we have

$$\mathbf{U} = \mathbf{F}_{MN}^{\mathbf{H}}\mathbf{Q}^{\mathbf{H}}\mathbf{F}_{MN}\mathbf{F}_{MN}^{\mathbf{H}}\mathbf{Q} = \mathbf{F}_{MN}^{\mathbf{H}}, \qquad (28)$$

and hence the condition (25) is satisfied. Therefore, the adaptive transmission system can be designed as shown in Fig. 4.

At the transmitter of the adaptive transmission, a sequence of data symbols $x[i]$, $i = 0, 1, ..., MN-1$ is converted to a vector $\mathbf{x}$ via S/P. After transforming $\mathbf{x}$ into the frequency-domain by FFT, the frequency-domain symbol vector is pre-coded by the eigenvector matrix $\mathbf{Q}$. After converting the frequency-domain precoded symbol vector to time-domain by IFFT and appending the cyclic prefix (CP), the data symbol frame is sent over the fast fading channel. At the receiver, after the CP removal and channel estimation, the CSI is fed-back to the transmitter and the received signal is recovered by the MMSE equalization. The recovered frequency-domain symbol vector can be expressed as

$$\mathbf{Y} = \mathbf{Q}^{\mathbf{H}}\mathbf{G}_{\nu}\mathbf{H}_{\nu}\mathbf{Q}\mathbf{X} + \mathbf{Q}^{\mathbf{H}}\mathbf{G}_{\nu}\mathbf{W}, \qquad (29)$$

which indicates that the adaptive transmission system performs all the precoding, equalization and decoding processes in the frequency-domain. Hence, the proposed adaptive transmission system is a kind of adaptive precoded OFDM system.

Since the output SNR of each data becomes the same with adaptive transmission, the BER can be simplified as

$$P_b = E_h\{\frac{2(1-2^{-k})}{k}Q(\sqrt{\frac{3}{4^k-1}\gamma_{out}^*})\}, \qquad (30)$$

B. BER Bounds Analysis

Under some extreme channel conditions with respect to the number of multipaths and maximum Doppler frequency shift, the performance bounds for the adaptive transmission scheme can be obtained analytically as follows.

1) Lower Bound: The first extreme channel condition is set as a channel with a fixed Doppler frequency shift in every multipaths, which can be regarded as a slow fading channel after the Doppler frequency shift is compensated. For such a channel, the time-domain channel matrix is a circulant matrix and can be transformed into diagonal matrix in the frequency-domain by 2D FT, which can be expressed as

$$\mathbf{H}_{\nu} = \mathbf{F}_{MN}^{\mathbf{H}}\mathrm{diag}(\alpha_i)\mathbf{F}_{MN}, \qquad (31)$$

where α_i, $i = 0, 1, ..., MN-1$, denotes the fading coefficient at frequency bin i. From (21), we can obtain

$$\mathbf{\Lambda} = \mathrm{diag}(\lambda_i) = \mathrm{diag}(\alpha_i)^{\mathbf{H}}\mathrm{diag}(\alpha_i) = \mathrm{diag}(|\alpha_i|^2). \qquad (32)$$

Assuming that all multipaths are independent, α_i are zero-mean independent complex Gaussian variables. When P approaches infinity, $\lambda_i = |\alpha_i|^2$ obeys chi-square distribution with two degrees of freedom and the probability density function (PDF) $e^{-\rho}$. In this condition, the normalized noise power for the equalized data symbol in the adaptive transmission can be evaluated from (26) as

$$J_{low} = \int_0^{\infty} \frac{e^{-\rho}}{\gamma_{in}\rho + 1} \, d\rho = E_1(\frac{1}{\gamma_{in}})e^{\frac{1}{\gamma_{in}}}, \qquad (33)$$

where $E_1\{\cdot\}$ is the exponential integral function, which is defined as

$$E_1(z) = \int_z^{\infty} \frac{e^{-t}}{t} \, dt. \qquad (34)$$

The output SNR can be expressed as

$$\begin{aligned}\gamma_{low} &= \frac{1}{J_{low}} - 1 \\ &= \frac{\gamma_{in}}{E_1(\frac{1}{\gamma_{in}})e^{\frac{1}{\gamma_{in}}}} - 1, \qquad (35)\end{aligned}$$

Thus, the lower bound of the BER performance can be obtained as

$$P_{b,low} = Q\left(\sqrt{\frac{\gamma_{in}}{E_1(\frac{1}{\gamma_{in}})e^{\frac{1}{\gamma_{in}}}} - 1}\right). \qquad (36)$$

2) Upper Bound: The second extreme channel condition considers the case when Doppler frequencies are uniformly distributed over $[-K_{max}, K_{max}]$, and $K_{max} \to \infty$. Supposing there are a large number of multipaths in the channel, the channel matrix in the frequency-domain $\mathbf{H}_{\nu}$ becomes a random matrix, whose entries obey independent Gaussian distribution with zero mean and unit variance. Therefore, the entries of the Hermitian matrix $\mathbf{H}_{\nu}^{\mathbf{H}}\mathbf{H}_{\nu}$ obey the complex Wishart distribution. The eigenvalues of $\mathbf{H}_{\nu}^{\mathbf{H}}\mathbf{H}_{\nu}$ have a PDF $\frac{1}{2\pi}\sqrt{\frac{4-\rho}{\rho}}$, $0 \leqslant \rho \leqslant 4$. Under this condition, the normalized

noise power for the equalized data symbol under the adaptive transmission can be expressed as

$$J_{up} = \int_0^4 \frac{\frac{1}{2\pi}\sqrt{\frac{4-\rho}{\rho}}}{\gamma_{in}\rho + 1} \, d\rho$$
$$= \frac{\sqrt{4\gamma_{in}+1}-1}{2\gamma_{in}}, \qquad (37)$$

and the output SNR can be expressed as

$$\gamma_{up} = \frac{1}{J_{up}} - 1$$
$$= \frac{2\gamma_{in}}{\sqrt{4\gamma_{in}+1}-1} - 1. \qquad (38)$$

The upper bound of the BER performance can be obtained as

$$P_{b,up} = Q\left(\sqrt{\frac{2\gamma_{in}}{\sqrt{4\gamma_{in}+1}-1} - 1}\right). \qquad (39)$$

We know that the system performance and diversity orders in fast fading channels depend on the number of multipaths and the maximum Doppler frequency shift. For the OTFS modulation, it is hard to derive a closed-form expression of the BER performance based on MMSE equalization given arbitrary numbers of multipaths and Doppler frequency shifts. However, for the proposed adaptive transmission, the theoretical BER bounds are available because the precoding $\mathbf{Q}$ matrix can simplify the channel matrix into a diagonal matrix. After applying an asymptotic method under the conditions that some system parameters are set to extreme values, the adaptive transmission can be adopted to verify the theoretical limits of a general precoded OFDM system with MMSE equalization in fast fading channels.

V. SIMULATION RESULTS

In this section, simulations are performed to compare the OTFS performance with the performance bounds. Assuming that the same amount of data are transmitted, some traditional short-frame modulations, such as OFDM and SC-FDE, are also compared. We consider OTFS as a long-frame modulation since OTFS needs Doppler frequency shifts with sufficient resolution and at the same time requires sufficient number of subcarriers to cope with the multipath propagation. On the contrary, short-frame modulations are proper transmission schemes in multipath channels but with lower Doppler resolutions. Two channel models are considered with diverse impulse response in the following simulations. To be specific, ETSI's channel models with non-equal-power channel taps are adopted for assessing the adaptive transmission performance, and the equal-power multipath channel model is adopted for evaluating the diversity performance. We also use 4-QAM as the symbol mapping technique except for the case when 16-QAM is used for comparison purpose.

TABLE I
SIMULATION PARAMETERS

Carrier Frequency (f_c)	No. of Subcarriers (M)	No. of OFDM/SC-FDMA Symbols (N)
6 GHz	256	32
Subcarrier Spacing (f_Δ)	Bandwidth ($W = Mf_\Delta$)	Duration of OFDM/SC-FDMA Symbol ($T = M/W$)
30 KHz	7.68 MHz	33.33 μs
Delay Resolution ($d_r = 1/W$)	Doppler Resolution ($f_r = 1/NT$)	Maximum Speed (v_{max})
130.21 ns	937.5 Hz	500 Km/h
Maximum Doppler Frequency ($f_{max} = f_c\frac{v_{max}}{v_c}$, $v_c = 3 \times 10^8$ m/s)	No. of Doppler Shifts (Positive or Negative) ($K_{max} = \left\lceil\frac{f_{max}}{f_r}\right\rceil$)	No. of Multipaths ($L_{max} = \left\lceil\frac{d_{max}}{d_r}\right\rceil$)
2777.8 Hz	≈ 3	≈ 35(LOS), 27(NLOS)

A. Adaptive Transmission Performance and Comparison

Firstly, let us compare the performance of adaptive transmission with OTFS and other conventional modulations. Here, we adopt the tapped delay line (TDL) channel models recommended by ETSI [32], [33], in which the time delays and channel gains in all multipath taps are defined in line-of-sight (LOS) and non-line-of-sight (NLOS) conditions. To simulate a fast fading channel, Doppler frequency shifts which obey uniform distribution ranging from $-K_{max}$ to K_{max} are applied. All the parameters are listed in Table I, in which d_{max} indicates the maximum delay time cited from [32]. Both short and long frame transmissions are compared. For long-frame modulations, including OTFS and Adaptive-long, there are MN data symbols in one frame. For short-frame modulations, including OFDM, SC-FDE and Adaptive-short, there are M data symbols in one frame.

The performance comparison is made based on the simulated BERs for different modulations under the above described LOS and NLOS channel conditions with fast fading. For each realization of the fast fading channel, a sufficient number of signal frames are generated with the specified modulation. After passing through the channel, the received signals are corrupted by AWGN according to a given SNR level. With perfect synchronization and known CSI, frequency-domain MMSE equalization is then performed using the equalization matrix defined in (18). The detected information bits are compared with the transmitted ones and the number of error bits are recorded. After 1000 iterations of random channel realizations, the average BER is finally obtained.

Note that the computational complexity of the adopted frequency-domain MMSE equalization is $O((1 + 4K_{max})^2 MN)$ in terms of the number of complex multiplications and divisions, where MN is the length of the signal frame. For conventional MMSE equalization without
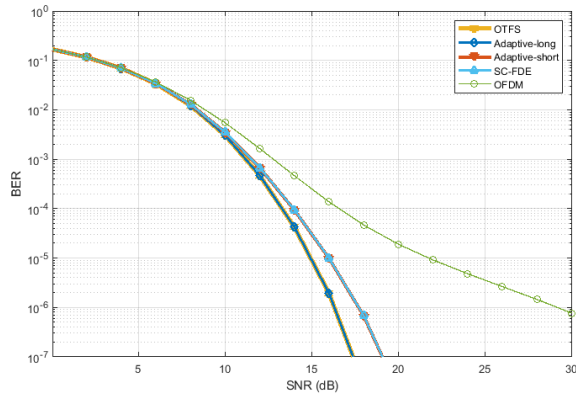
Fig. 5. Comparison of various modulation schemes in LOS channels.

Fig. 6. Comparison of various modulation schemes with and without channel estimation error in NLOS channels.

exploring the stripe diagonal structure of frequency-Doppler domain channel matrix, the computational complexity is $O((MN)^3)$. As the equalization is performed in the frequency domain, the complexity only depends on K_{max} but not the number of multipath. Under the ETSI NLOS channels specified in Table I, the computational complexity for MMSE equalization is $O(169MN)$, while the computational complexity for Message Passing is $O(2700MNn_{iter})$, where n_{iter} is the number of iterations. It is evident that the frequency-domain MMSE equalization is superior to MP in terms of complexity. On the other hand, an iterative decision feedback equalizer (DFE) proposed in [34] achieves $O(NML)$ per iteration, where L is the number of delay taps. As a time-domain approach, it is an attractive solution in channels with less multipath, whereas our method is more suitable when the channel has a smaller Doppler spread.

Fig. 5 shows the BER performance in LOS channel. Note that OTFS and Adaptive-long demonstrate similar performance, achieving 10^{-7} BER at SNR around 17 dB. SC-FDE and Adaptive-short incur about 2 dB degradation. OFDM shows the worst performance, lagging far behind others.

Fig. 6 shows the BER performance in NLOS channels. We first compare different modulations with perfectly known CSI (legends with prefix "P-"). We see that P-Adaptive-long demonstrates the best performance and achieves 10^{-7} BER at SNR about 24 dB, outperforming OTFS by about 4 dB. For the short frame modulations, although the P-Adaptive-short performs worse than long frame modulations, it can still achieve a BER of 10^{-7} at about 30 dB and is much better than SC-FDE and OFDM.

To prove that adaptive transmission is effective in practice, simulations are also conducted with CSI not perfectly known at the receiver (legends with prefix "I-"). In doing so, a random matrix obeying Gaussian distribution for each element is added into the estimated channel matrix [35]. Assuming the variance of channel error is inversely proportional to the SNR, both Adaptive-long and OTFS, denoted as I-Adaptive-long and I-OTFS, are simulated and the results are shown in Fig. 6. We observe that the impact of channel estimation error on the performance is significant in a lower SNR region but tends to be minor in a higher SNR region. Meanwhile, adaptive
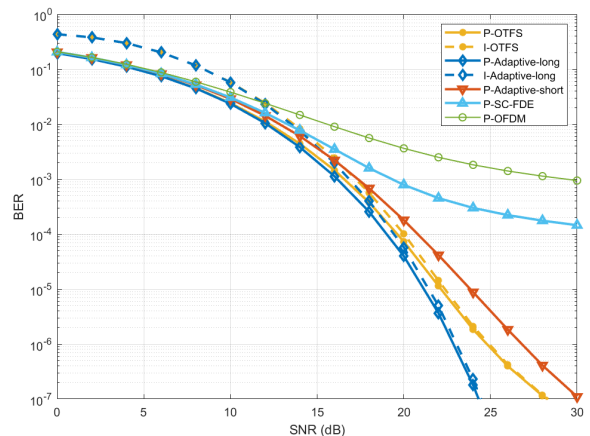
transmission keeps showing better performance than OTFS.

It is worthwhile noting that, in LOS channels, SC-FDE and Adaptive-short show very close performance to long-frame modulations. In NLOS channels, with the help of precoding, the short-frame adaptive transmission demonstrates much better performance than short-frame modulations, close to those of long-frame modulations. This result confirms that the adaptive precoding can indeed improve the performance of short-frame modulations, and the adaptive transmission with short frames provides a practical solution considering its low complexity and short delay in signal processing.

The results in Figs. 5 and 6 also show how the BER performance is impacted by diversities in different domains. Firstly, long-frame modulations can exploit both time and frequency diversity so that they achieve the best performance. Then, SC-FDE can exploit frequency diversity but only partially resolve the Doppler frequency so that it shows degraded performance. Finally, conventional OFDM without precoding can not exploit frequency diversity so that it shows the worst performance.

The BER performance for 16-QAM is also simulated to verify the effect of precoding. As shown in Fig. 7, the adaptive transmission and OTFS modulations with 16-QAM demonstrate similar trends to those with 4-QAM in both LOS and NLOS channels. Therefore, the proposed adaptive transmission is also an effective solution to combating fast fading channels for signals with higher order modulation levels.

The peak to average power ratios (PAPRs) of the OTFS with and without precoding are also simulated. The results show that the OTFS without precoding has lower PAPR than OFDM and the adaptive transmission. The PAPRs of the adaptive transmission and OFDM are very similar, and are only about 0.5 dB higher than that of OTFS, when the probability of PAPR greater than a specified threshold is 10^{-5}. It proves that the impact of precoding on PAPR performance is negligible.

B. BER Bounds Validation

After the performance of the adaptive transmission is verified, we now validate the BER upper and lower bounds
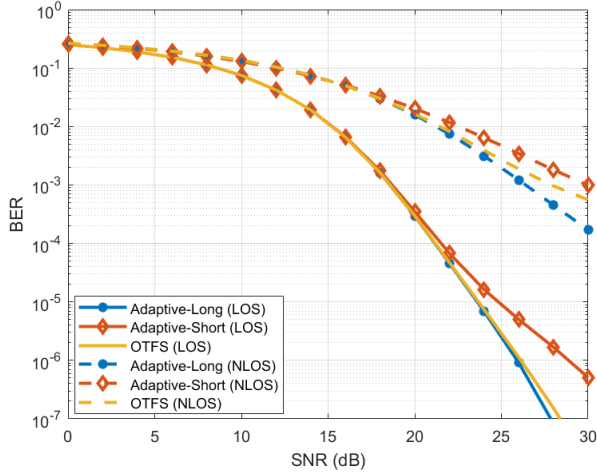
Fig. 7. Comparison of various modulation schemes with 16-QAM under both LOS and NLOS channels.

Fig. 9. Upper bounds of MMSE equalization performance under different Doppler frequency diversity orders with $P = M \times N$. The curves from left to right correspond to $K_{max} = 1, 4, 64$, and asymptotic ∞.
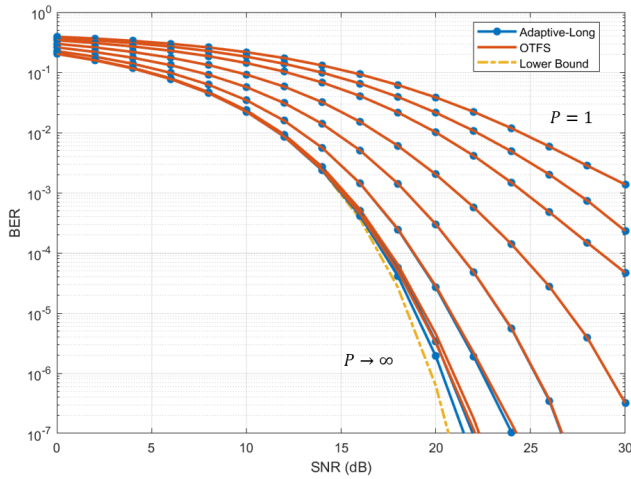

Fig. 8. Lower bounds of MMSE equalization performance under different multipath diversity orders without Doppler frequency shifts. The curves from right to left correspond to $P = 1, 2, 4, 8, 16, 32, 64, 128, 1024$, and asymptotic ∞.

Fig. 10. BER comparison under adaptive transmission when $K_{max} = 1, 4, 16, 64$ in high SNR region.

using MMSE equalization. The BER bounds between adaptive transmission and OTFS are compared under some extreme channel conditions. We adopt larger P or K_{max} in these simulations and assume that the channel has equal-power for each multipath, while other parameters remain the same as in Table I. To consider more practical conditions, we use the ETSI channel models as described in Section V.A, which have relatively smaller P.

Fig. 8 shows the BER performance comparison under varying multipath diversity orders. We observe that the performance is improved as P increases. When $P \to \infty$, the performance of adaptive transmission converges towards the theoretical lower bound, which achieve 10^{-7} BER at SNR about 20.5 dB. The OTFS curves nearly overlap with those of the adaptive transmission when P is small, but gaps appear as P becomes large.

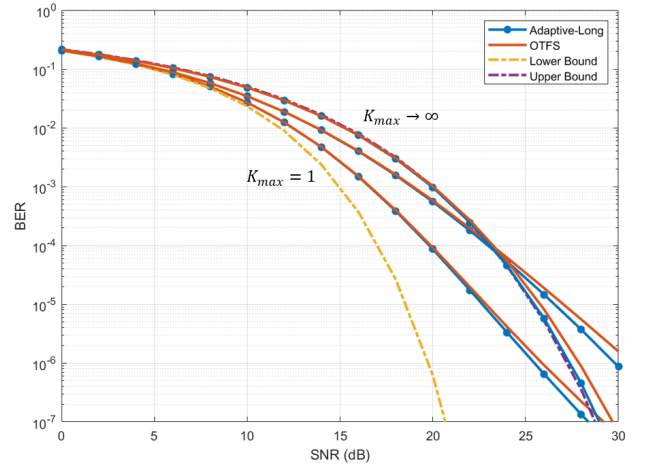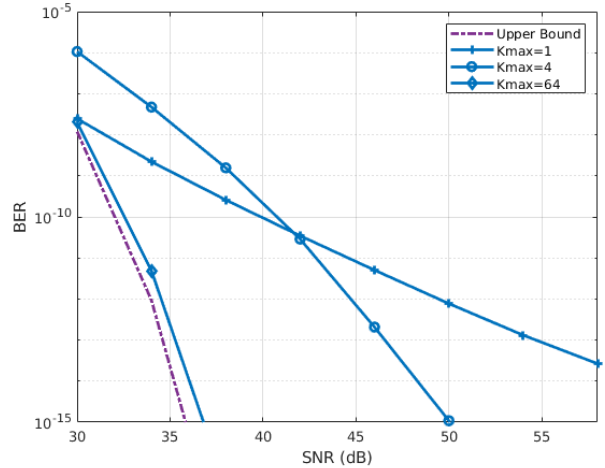Fig. 9 shows the BER performance comparison under vary-

ing Doppler frequency shifts with $K_{max} = 1, 4, 64$, and ∞ when P is set to MN. It is well-known that the diversity performance is represented by the slope of the BER performance curve when the SNR tends to infinity. After enlarging the SNR range, it can be seen from Fig. 10 that the diversity orders of adaptive transmission increase as K_{max} increases. However, this does not mean that the actual BERs will be reduced in a low SNR region as the diversity order increases. In fact, from Fig. 9, the BER performance under smaller Doppler diversity orders is superior to those with larger Doppler diversity orders in a low SNR region. Considering the more practical BER comparison in a low SNR region, we still use the term upper bound to describe the BER performance when $K_{max} \to \infty$, though the Doppler diversity is not upper bounded by it. Above simulation results reveal a very interesting property of the adaptive transmission in terms of the relationship between Doppler diversity order and BER performance, which we have never seen in the literature.

Note that in a practical channel condition the number of multipaths or the maximum Doppler frequency shift will not be infinite but the analytical performance bounds can serve as benchmarks for practical system design. In some application scenarios, the number of multipaths can be very large, such as in the urban macro (UMa) channel. In the emerging ISTNs which involve aircraft-to-aircraft and aircraft-to-ground communications, the Doppler frequency shift can also be very large. Therefore, the analysis of BER bounds is of great significance.

Overall, although the performance of the two techniques are very close, our proposed adaptive transmission is superior to OTFS under all simulated conditions. It also proves that OTFS can achieve almost optimal performance in fast fading channels. Though the lower and upper bounds are derived for the proposed adaptive transmission, they can also serve as the performance benchmarks for OTFS systems.

VI. Conclusions

In this paper, we have formulated OTFS as a precoded OFDM and applied frequency-domain channel models and signal processing to analyze its diversity performance in fast fading channels. With low complexity MMSE equalization, an adaptive transmission scheme is proposed to optimize the the diversity performance. Two BER bounds are derived by considering two extreme channel conditions. These bounds can serve as the benchmarks for OTFS and adaptive transmission systems. The simulation results show that the adaptive transmission achieves the best performance in fast fading channels. It is also demonstrated that the proposed adaptive transmission is very effective for short signal frames and is robust to channel estimation errors. Our future work includes the investigation of further complexity-reduced equalization techniques, such as the iterative decision feedback equalizer in the frequency domain, for adaptive transmission over fast fading channels.

Appendix A

From (1) and (3), the received signal can be expressed as

$$r(t) = \int_{-\infty}^{+\infty} h_t(\tau, t) s(t - \tau) d\tau + w(t). \qquad (40)$$

In the discrete-time domain, it becomes

$$r[i] = \sum_{j=-\infty}^{+\infty} h_t[j, i] s[i - j] + w[i], \qquad (41)$$

where $h_t[j, i]$ and $w[i]$ are the discrete-time versions of the delay-time channel representation $h_t(\tau, t)$ and noise $w(t)$, respectively sampled at $t = i d_r$ and $\tau = j d_r$. We assume that the transmitted data symbols $s[0], s[1], ..., s[MN - 1]$ are independent with equal power σ_s^2 and the noise power is σ_w^2. After OTFS demodulation, i.e., Wigner transform followed by symplectic finite Fourier transform (SFFT), the $(m'M + m)$-th recovered signal can be expressed as

$$y[m'M + m] = \sum_{n=0}^{N-1} r[nM + m] e^{-\mathbf{j}\frac{2\pi}{N}nm'}, \qquad (42)$$

for $m' = 0, ..., N - 1$, $m = 0, ..., M - 1$,. To calculate the output SNR, the power of $y[m'M + m]$ can be expressed as

$$\mathbf{E}\{|y[m'M + m]|^2\}$$
$$= \mathbf{E}\{\sum_{n=0}^{N-1} r[nM + m] e^{-\mathbf{j}\frac{2\pi}{N}nm'} \sum_{n'=0}^{N-1} r^*[n'M + m] e^{\mathbf{j}\frac{2\pi}{N}n'm'}\}$$
$$= \sum_{n=0}^{N-1}\sum_{n'=0}^{N-1} \mathbf{E}\{r[nM + m] r^*[n'M + m]\} e^{\mathbf{j}\frac{2\pi}{N}(n'-n)m'}, \qquad (43)$$

where $(\cdot)^*$ denotes the complex conjugation. Supposing that $M > L$ where L is the maximum multipath delay, Eq. (43) can be simplified as (44) since $\mathbf{E}\{r[nM + m] r^*[n'M + m]\} = 0$, for $n \neq n'$. Based on Eq. (3), we also assume that the relationship between $h_t[l, j]$ and $h[l, k]$ is

$$h_t[l, j] = \frac{1}{\sqrt{MN}} \sum_{k=-K_{max}}^{K_{max}} h[l, k] e^{\mathbf{j}\frac{2\pi}{MN}kj}. \qquad (45)$$

From (44) and ignoring any scaling factor, the output SNR can be expressed as shown in (16).

References

[1] X. Huang, J. A. Zhang, R. P. Liu, Y. J. Guo, and L. Hanzo, "Airplane-aided integrated networking for 6G wireless: Will it work?" *IEEE Vehicular Technology Magazine*, vol. 14, no. 3, pp. 84–91, Sep. 2019.

[2] J. Liu, Y. Shi, Z. M. Fadlullah, and N. Kato, "Space-air-ground integrated network: A survey," *IEEE Communications Surveys Tutorials*, vol. 20, no. 4, pp. 2714–2741, Fourthquarter 2018.

[3] B. Aazhang, P. Ahokangas, H. Alves, M.-S. Alouini, J. Beek, H. Benn, M. Bennis, J. Belfiore, E. Strinati, F. Chen, K. Chang, F. Clazzer, S. Dizit, K. DongSeung, M. Giordiani, W. Haselmayr, J. Haapola, E. Hardouin, E. Harjula, and P. Zhu, "Key drivers and research challenges for 6G ubiquitous wireless intelligence (white paper)," September 2019. [Online]. Available: http://jultika.oulu.fi/files/isbn9789526223544.pdf

[4] Yuping Zhao and S. . Haggman, "Intercarrier interference self-cancellation scheme for OFDM mobile communication systems," *IEEE Transactions on Communications*, vol. 49, no. 7, pp. 1185–1191, July 2001.

[5] K. Lin, H. Lin, and M. Tseng, "An equivalent channel time variation mitigation scheme for ICI reduction in high-mobility OFDM systems," *IEEE Transactions on Broadcasting*, vol. 58, no. 3, pp. 472–479, Sep. 2012.

[6] X. Gao, L. Dai, Y. Zhang, T. Xie, X. Dai, and Z. Wang, "Fast channel tracking for terahertz beamspace massive MIMO systems," *IEEE Transactions on Vehicular Technology*, vol. 66, no. 7, pp. 5689–5696, July 2017.

[7] W. Wang and S. S. Abeysekera, "Data aided phase tracking and symbol detection for CPM in frequency-flat fading channel," in *2011 IEEE International Conference on Acoustics, Speech and Signal Processing (ICASSP)*, May 2011, pp. 3500–3503.

[8] S. Stefanatos and A. K. Katsaggelos, "Joint data detection and channel tracking for OFDM systems with phase noise," *IEEE Transactions on Signal Processing*, vol. 56, no. 9, pp. 4230–4243, Sep. 2008.

[9] H. Nguyen-Le and T. Le-Ngoc, "Pilot-aided joint CFO and doubly-selective channel estimation for OFDM transmissions," *IEEE Transactions on Broadcasting*, vol. 56, no. 4, pp. 514–522, Dec 2010.

[10] H. Nguyen-Le, T. Le-Ngoc, and N. H. Tran, "Iterative receiver design with joint doubly selective channel and CFO estimation for coded MIMO-OFDM transmissions," *IEEE Transactions on Vehicular Technology*, vol. 60, no. 8, pp. 4052–4057, Oct 2011.

[11] W. Chin, "Nondata-aided doppler frequency estimation for OFDM systems over doubly selective fading channels," *IEEE Transactions on Communications*, vol. 66, no. 9, pp. 4211–4221, Sep. 2018.

[12] E. P. Simon and M. A. Khalighi, "Iterative soft-Kalman channel estimation for fast time-varying MIMO-OFDM channels," *IEEE Wireless Communications Letters*, vol. 2, no. 6, pp. 599–602, December 2013.

$$\mathbf{E}\{|y[m'M + m]|^2\}$$
$$= \sum_{n=0}^{N-1} \mathbf{E}\{|r[nM + m]|^2\}$$
$$= \sum_{n=0}^{N-1} \sum_{l=0}^{L-1} |h_t[l, nM + m]|^2 \sigma_s^2 + \sigma_w^2$$
$$= \frac{1}{MN} \sum_{n=0}^{N-1} \sum_{l=0}^{L-1} \sum_{k=-K_{max}}^{K_{max}} \sum_{k'=-K_{max}}^{K_{max}} h[l, k] e^{\mathbf{j}\frac{2\pi}{MN} k(nM+m)} h^*[l, k'] e^{-\mathbf{j}\frac{2\pi}{MN} k'(nM+m)} \sigma_s^2 + \sigma_w^2$$
$$= \frac{1}{M} \sum_{l=0}^{L-1} \sum_{k=-K_{max}}^{K_{max}} |h[l, k]|^2 \sigma_s^2 + \sigma_w^2$$

(44)

[13] S. Ahmed, M. Sellathurai, S. Lambotharan, and J. A. Chambers, "Low-complexity iterative method of equalization for single carrier with cyclic prefix in doubly selective channels," *IEEE Signal Processing Letters*, vol. 13, no. 1, pp. 5–8, Jan 2006.

[14] R. Hadani, S. Rakib, M. Tsatsanis, A. Monk, A. J. Goldsmith, A. F. Molisch, and R. Calderbank, "Orthogonal time frequency space modulation," in *2017 IEEE Wireless Communications and Networking Conference (WCNC)*, March 2017, pp. 1–6.

[15] R. Hadani, S. Rakib, A. F. Molisch, C. Ibars, A. Monk, M. Tsatsanis, J. Delfeld, A. Goldsmith, and R. Calderbank, "Orthogonal time frequency space (OTFS) modulation for millimeter-wave communications systems," in *2017 IEEE MTT-S International Microwave Symposium (IMS)*, June 2017, pp. 681–683.

[16] K. R. Murali and A. Chockalingam, "On OTFS modulation for high-Doppler fading channels," in *2018 Information Theory and Applications Workshop (ITA)*, San Diego, CA, USA, Feb 2018.

[17] P. Raviteja, K. T. Phan, Y. Hong, and E. Viterbo, "Interference cancellation and iterative detection for orthogonal time frequency space modulation," *IEEE Transactions on Wireless Communications*, vol. 17, no. 10, pp. 6501–6515, Oct 2018.

[18] P. Raviteja, K. T. Phan, Q. Jin, Y. Hong, and E. Viterbo, "Low-complexity iterative detection for orthogonal time frequency space modulation," in *2018 IEEE Wireless Communications and Networking Conference (WCNC)*, Barcelona, Spain, April 2018.

[19] P. Raviteja, Y. Hong, E. Viterbo, and E. Biglieri, "Practical pulse-shaping waveforms for reduced-cyclic-prefix OTFS," *IEEE Transactions on Vehicular Technology*, vol. 68, no. 1, pp. 957–961, Jan 2019.

[20] P. Raviteja, E. Viterbo, and Y. Hong, "OTFS performance on static multipath channels," *IEEE Wireless Communications Letters*, vol. 8, no. 3, pp. 745–748, June 2019.

[21] S. Tiwari, S. S. Das, and V. Rangamgari, "Low complexity LMMSE receiver for OTFS," *IEEE Communications Letters*, vol. 23, no. 12, pp. 2205–2209, 2019.

[22] F. Long, K. Niu, C. Dong, and J. Lin, "Low complexity iterative LMMSE-PIC equalizer for OTFS," in *ICC 2019 - 2019 IEEE International Conference on Communications (ICC)*, May 2019, pp. 1–6.

[23] T. Thaj and E. Viterbo, "Low complexity iterative rake detector for orthogonal time frequency space modulation," in *2020 IEEE Wireless Communications and Networking Conference (WCNC)*, 2020, pp. 1–6.

[24] G. D. Surabhi and A. Chockalingam, "Low-complexity linear equalization for 2×2 MIMO-OTFS signals," in *2020 IEEE 21st International Workshop on Signal Processing Advances in Wireless Communications (SPAWC)*, 2020, pp. 1–5.

[25] P. Raviteja, Y. Hong, E. Viterbo, and E. Biglieri, "Effective diversity of OTFS modulation," *IEEE Wireless Communications Letters*, vol. 9, no. 2, pp. 249–253, Feb 2020.

[26] E. Biglieri, P. Raviteja, and Y. Hong, "Error performance of orthogonal time frequency space (OTFS) modulation," in *2019 IEEE International Conference on Communications Workshops (ICC Workshops)*, Shanghai, China, May 2019.

[27] G. D. Surabhi, R. M. Augustine, and A. Chockalingam, "On the diversity of uncoded OTFS modulation in doubly-dispersive channels," *IEEE*

[28] F. Hlawatsch and G. Matz, *Wireless Communications Over Rapidly Time-Varying Channels*, 1st ed. Orlando, FL, USA: Academic Press, Inc., 2011.

[29] Xiaojing Huang, "Diversity performance of precoded OFDM with MMSE equalization," in *2007 International Symposium on Communications and Information Technologies*, Oct 2007, pp. 802–807.

[30] X. Huang, "Multipath diversity of precoded OFDM with linear equalization," in *2008 IEEE International Conference on Communications*, May 2008, pp. 1307–1311.

[31] J. Proakis and M. Salehi, *Digital Communications*, 5th ed. McGraw-Hill.

[32] ETSI, "Study on channel model for frequencies from 0.5 to 100 GHz," *ETSI TR 138 901 V15.0.0*, July 2018.

[33] ——, "Base Station (BS) radio transmission and reception," *ETSI TS 138 104 V15.2.0*, July 2018.

[34] T. Thaj and E. Viterbo, "Low complexity iterative rake decision feedback equalizer for zero-padded OTFS systems," *IEEE Transactions on Vehicular Technology*, vol. 69, no. 12, pp. 15 606–15 622, 2020.

[35] S. Sharma, K. Deka, and B. Beferull-Lozano, "Low-complexity detection for uplink massive MIMO SCMA systems," *IET Communications*, no. 15(1), pp. 51–59, 2020.

Transactions on Wireless Communications, vol. 18, no. 6, pp. 3049–3063, June 2019.

Hongyang Zhang received the B. Eng and M. Eng degrees in control science and engineering from Xi'an JiaoTong University, China, in 2015 and 2018. He is currently pursuing his Ph.D. degree with Global Big Data Technologies Center, University of Technology Sydney, Australia. His current research interests include channel equalization and estimation, waveform designs for next generation wireless systems.

Xiaojing Huang (M'99-SM'11) received the B.Eng., M.Eng., and Ph.D. degrees in electronic engineering from Shanghai Jiao Tong University, Shanghai, China, in 1983, 1986, and 1989, respectively. He was a Principal Research Engineer with the Motorola Australian Research Center, Botany, NSW, Australia, from 1998 to 2003, and an Associate Professor with the University of Wollongong, Wollongong, NSW, Australia, from 2004 to 2008. He had been a Principal Research Scientist with the Commonwealth Scientific and Industrial Research Organisation (CSIRO), Sydney, NSW, Australia, and the Project Leader of the CSIRO Microwave and mm-Wave Backhaul projects since 2009. He is currently a Professor of Information and Communications Technology with the School of Electrical and Data Engineering and the Program Leader for Mobile Sensing and Communications with the Global Big Data Technologies Center, University of Technology Sydney (UTS), Sydney, NSW, Australia. His research interests include high-speed wireless communications, digital and analog signal processing, and synthetic aperture radar imaging. With over 32 years of combined industrial, academic, and scientific research experience, he has authored over 330 book chapters, refereed journal and conference papers, major commercial research reports, and filed 31 patents. Prof. Huang was a recipient of the CSIRO Chairman's Medal and the Australian Engineering Innovation Award in 2012 for exceptional research achievements in multigigabit wireless communications.

J. Andrew Zhang (M'04-SM'11) received the B.Sc. degree from Xi'an JiaoTong University, China, in 1996, the M.Sc. degree from Nanjing University of Posts and Telecommunications, China, in 1999, and the Ph.D. degree from the Australian National University, in 2004.

Currently, Dr. Zhang is an Associate Professor in the School of Electrical and Data Engineering, University of Technology Sydney, Australia. He was a researcher with Data61, CSIRO, Australia from 2010 to 2016, the Networked Systems, NICTA, Australia from 2004 to 2010, and ZTE Corp., Nanjing, China from 1999 to 2001. Dr. Zhang's research interests are in the area of signal processing for wireless communications and sensing. He has published more than 200 papers in leading international Journals and conference proceedings, and has won 5 best paper awards. He is a recipient of CSIRO Chairman's Medal and the Australian Engineering Innovation Award in 2012 for exceptional research achievements in multi-gigabit wireless communications. He is serving as an Editor for IEEE Trans. on Communications.